Carbohydrate Polymers 84 (2011) 1252–1257

Contents lists available at ScienceDirect

Carbohydrate Polymers

journal homepage: www.elsevier.com/locate/carbpol

Carbon black immobilized in electrospun chitosan membranes

Jessica D. Schiffman, Adam C. Blackford, Ulrike G.K. Wegst, Caroline L. Schauer*

Department of Materials Science and Engineering, Drexel University, Philadelphia, PA 19104, USA

ARTICLE INFO

Article history:
Received 7 July 2010
Received in revised form
20 December 2010
Accepted 11 January 2011
Available online 18 January 2011

Keywords:
Carbon black composites
Chitosan
Conductive nanofibers
Chitosan
Electrospinning
Fibers
Membranes

ABSTRACT

Cross-linked, non-woven fibrous membranes were successfully electrospun from carbon black–chitosan solutions. Morphology changes with increasing amounts of carbon black were analyzed by field emission scanning electron microscopy (FESEM). Chemical structure, conductance, and crystallinity of the fibrous membranes were investigated by Fourier transform infrared spectroscopy (FTIR), AC impedance spectroscopy, and X-ray diffraction (XRD), respectively. We hypothesize that even at 62.5 wt% loading of carbon black the particles are chelated and immobilized within the fibers by the natural polymer, chitosan. After cross-linking using glutaraldehyde vapor, all carbon black–chitosan membranes exhibited chemical stability in aqueous, acidic, and basic solutions for at least 20 days.

1. Introduction

Electrodes, electromagnetic interference (EMI) shielding, and sensors (Chen, Hu, Zhang, Li, & Rong, 2004; Doleman, Lonergan, Severin, Vaid, & Lewis, 1998; Zhang & Zeng, 1997) would benefit from the development of ultra-thin, flexible, electrically conductive natural polymer coatings. One way to fabricate such a coating is by electrospinning, an inexpensive, scalable process wherein electrical forces are utilized to create nano- to macro- sized non-woven membranes from a wide range of precursor materials (Schiffman & Schauer, 2008).

Previously, the morphology, mechanical behavior, electrical conductivity, and thermal resistance of electrospun synthetic polymer–carbon black membranes were evaluated (Chuangchote, Sirivat, & Supaphol, 2007; Hwang, Muth, & Ghosh, 2007). Additionally, synthetic polymer–carbon black membranes were evaluated as flexible strain sensors for non-cyclic strain sensing and to demonstrate a thermally induced color change (Pedicini & Farris, 2004; Tiwari, Yarin, & Megaridis, 2008). To date, only medium loadings (12.25 wt% or less) of carbon black have been successfully electrospun in synthetic polymer matrices.

As the concentration of carbon black within a polymer matrix increases, an insulator–conductor transition takes place. This percolation threshold is the critical amount of filler that diminishes insulating properties and creates a continuously conductive network. Typically, being able to reduce the percolation threshold translates to lowering production costs, and improved mechanical properties. However, for the successful design of applications requiring immobilized carbon blacks or other carbonaceous materials, it is imperative to confirm that even upon high weight percent loadings of these materials, they will be retained within the polymer and not leach into the environment. Immobilization utilizing a known chelating agent, such as chitosan, as a matrix material is an excellent way to achieve this.

The natural polymer chitosan is biocompatible, biodegradable, and has aqueous adsorption capabilities. It is the *N*-deacetylated derivative of chitin, which is a linear polysaccharide, composed of *N*-acetyl-D-glucosamine (*N*-acetyl-2-amino-2-deoxy-D-glucopryanose) units linked by β-D (1→4) bonds. As a result of the deacetylation process, the chemical structure of chitosan has an abundance of free amine groups. This, and its high nitrogen content at 6.89%, make it an effective chelator (Krajewska, 2004; Kumar, 2000; Kurita, 2006; Rinaudo, 2006). To date, there are no reports on chitosan electrospun with any carbon filler agents.

In the current work, the electrospinning process was utilized to produce membranes with low (2.5 wt%), medium (6.25–25.0 wt%), and high (62.5 wt%) loadings of carbon black. Changes in the morphology of the fibrous membranes and the extent to which the carbon black was incorporated into the fibers were analyzed using scanning electron microscopy and chemical stability studies. Crystallinity and mechanical properties, as well as the conductivity of

* Corresponding author. Tel.: +1 215 895 6797; fax: +1 215 895 6760.
E-mail address: cschauer@coe.drexel.edu (C.L. Schauer).

0144-8617/$ – see front matter © 2011 Elsevier Ltd. All rights reserved.
doi:10.1016/j.carbpol.2011.01.013

both the polymeric solution and electrospun membranes were also determined.

2. Materials and methods

2.1. Materials

All compounds were used as received. Carbon black acetylene 100% compressed 99.9+% (metals basis) was purchased from Alfa Aesar (Ward Hill, MA). The supplier published an average particle size of 42.0 nm. Using FESEM micrographs and ImageJ 1.41 software (National Institutes of Health, Bethesda, MD) the average size of the carbon black particles was determined to be 66.9 ± 16.2 nm ($n = 50$). Glutaraldehyde (GA) (50% solution in water), 97% pure sodium hydroxide (NaOH), 99.7+% ACS, reagent-grade acetic acid, Reagent-Plus 99% trifluoroacetic acid (TFA), and medium molecular weight (190–310 kDa) chitosan were purchased from Sigma–Aldrich (St. Louis, MO). Using FTIR, chitosan was previously determined to be 83% deacetylated (Schiffman & Schauer, 2007).

2.2. Membrane fabrication

2.2.1. Solution preparation

Chitosan/TFA solutions (0.4 g/15 mL corresponding to 2.7% (w/v) solutions) were prepared with 0 g, 0.01 g, 0.025 g, 0.1 g, and 0.25 g carbon black per 0.4 g chitosan. Carbon black–chitosan wt% ratios correspond to 0%, 2.5%, 6.25%, 25.0%, and 62.0%. Solutions were mixed for 24 h on an Arma-Rotator A-1 (Bethesda, MD).

2.2.2. Solution conductivity

A CON 5110 conductivity meter (Oakton, Vernon Hills, IL) was utilized to determine the conductivity of solutions containing chitosan and various amounts of carbon black. Measurements were taken in triplicates. All solutions were made utilizing 1% TFA solutions because initial testing proved that solutions containing strong 100% TFA solutions damaged the probe of the conductivity meter.

2.2.3. Electrospinning

A previously described electrospinning apparatus was utilized (Schiffman & Schauer, 2007). Approximately, 4 mL of a prepared solution was loaded into a 5 mL Luer-Lok Tip syringe and a Precision Glide 21-gauge needle (Becton Dickinson & Co., Franklin Lakes, NJ) was attached. The syringe was then placed on an advancement pump (Harvard Apparatus, Plymouth Meeting, PA) that was clipped to the target, which was comprised of a copper plate wrapped in aluminum foil. These were held at a fixed distance – the separation distance – while a voltage was applied creating positive and negative anodes. The advancement pump expunged the polymer solution of interest at a constant rate as referred to in Section 3 as the advancement speed.

2.2.4. Cross-linking

A previously described method (Schiffman & Schauer, 2007) was utilized to cross-link the membranes after they were electrospun. To the bottom of an 11.43 cm × 7.62 cm × 5.08 cm vapor chamber (VWR Scientific Products, Bridgeport, NJ), 3 mL GA-liquid was added; the membranes were then placed in the chamber for 24 h.

2.3. Characterization of electrospun membranes

2.3.1. Microscopy

A Zeiss Supra 50/VP field emission scanning electron microscope (FESEM) was utilized to capture micrographs of the membranes. A Denton vacuum desk II sputtering machine coated the samples for 5 s with platinum–palladium. Average fiber diameter, where $n = 50$ from at least 5 different micrographs, was determined using ImageJ 1.41 software.

For samples that were focused ion beam (FIB) milled, a 1 μm layer of platinum was deposited locally to minimize ion beam damage; the cross-section was prepared with a 30 kV Ga^+-beam. FIB samples were then coated with a 15 nm layer of gold-palladium prior to imaging using a FEI Nova 600 Nanolab DualBeam system.

2.3.2. Chemical analysis

Infrared spectra for electrospun membranes before and after cross-linking were measured using attenuated reflectance Fourier transform infrared spectroscopy (FTIR) (Excalibur FTS-3000). All spectra were taken in transmission mode over the spectral range of 4000–500 cm^{-1} by accumulation of 64 scans at a resolution of 4 cm^{-1}.

The chemical stability of cross-linked membranes containing 0–62.5 wt%, carbon black was evaluated. 15-mm^2 petri dishes (Becton Dickinson, Franklin Lakes, NJ), each contained 30 mL basic solution (1 M NaOH, pH ~13) or acidic solution (1 M acetic acid, pH ~2) or aqueous solution (ultrapure water, pH ~7). Two, 2.54 cm × 1.27 cm samples were placed into each solution. If possible, one of the membranes was removed after 15 min, and the second observed after 48 h and then removed after 20 days. The solubility and integrity of the membranes over the time elapsed was visually inspected.

2.3.3. Crystallinity

A D500 Siemens X-ray diffractometer (XRD) with a Cu Kα source was utilized to obtain diffraction patterns of cross-linked membranes, which were mounted onto glass slides wrapped with store purchased aluminum (Al) foil (Schiffman, Stulga, & Schauer, 2009). Scans were taken from 5° to 30° with a hold time of 0.04 s. MDI JADE 7 software was used for peak detection and subtraction of Al foil peaks.

2.4. Evaluation of electrospun membranes

2.4.1. Conductivity

The conductivity of the plane normal to the electrospun membranes was measured utilizing AC impedance spectroscopy, using a Solartron AC Impedance system (1260 impedance analyzer, and 1287 electrochemical interface), which has previously been described (Elabd, Walker, & Beyer, 2004). A two-electrode cell was used comprised of 1.22 cm^2 stainless steel blocking electrodes. Zplot software was utilized to determine the resistance of the membranes within the AC frequency range of 100 Hz to 1 MHz. The values reported for electrical conductivity (σ) represent the average of three experiments, as determined according to the equation:

$$\sigma = \frac{l}{AR} \quad (1)$$

where R is the electrical resistivity (Ω), A is the cross-sectional area (cm^2), and l is the thickness of the membrane (cm). The thickness represents an average of three measurements taken utilizing a digital micrometer (Mitutoyo, Aurora, IL). Dry membranes were tested at room temperature (23 °C), where the relative humidity was 20%.

2.4.2. Uniaxial tensile testing

The Kawabata KES-G1 tabletop uniaxial testing machine was utilized to determine mechanical properties of dry electrospun membranes containing variable amounts of carbon black before and after cross-linking. Membranes measuring 5.0 cm × 0.5 cm were mounted in "C"-shaped holders that were cut prior to the application of a 0.02 s^{-1} strain rate. Young's modulus (MPa), ultimate break strain (%), and ultimate tensile strength (MPa) were calculated as previously described (Schiffman & Schauer, 2007). The

raw data was normalized by accounting for the areal density of each sample tested. The testing was conducted at room temperature (23 °C).

3. Results and discussion

3.1. Characteristics of carbon black–chitosan solutions

Numerous parameters – polymer, solution, operations – impact the electrospinability of a polymer solution (Schiffman & Schauer, 2008). Previously, various molecular weights and degrees of deacetylated chitosan have been electrospun utilizing the solvent, triflouroacetic acid (TFA). The conductivity (Figures S1 and S2) and viscosity of chitosan varies greatly depending on the given acid and its concentration since chitosan's degree of protonation depends on the pK_a of the acid used to solubilize the chitosan (Rinaudo, Pavlov, & Desbrières, 1999). TFA facilitates electrospinning as it forms salts with the amino groups on chitosan, which destroys the strong interaction between the chitosan molecules and allows for a critical polymer chain entanglement to ensue (Hasegawa, Isogai, Onabe, & Usuda, 1992; Schiffman & Schauer, 2007).

Applied voltage was held constant at 25 kV to electrospin all chitosan and carbon black–chitosan solutions; other system parameters had to optimized. While pure chitosan\TFA solutions electrospun with a needle-to-target separation distance and a solution advancement speed of 6.4 cm and 1.20 mL/h, respectively, carbon black–chitosan\TFA solutions required an increased separation distance of 16 cm and decreased advancement speed of 0.08 mL/h.

3.2. Characteristics of electrospun carbon black–chitosan membranes

Chitosan membranes were successfully electrospun with increasing amounts of carbon black incorporated as qualitatively confirmed by the dramatic color changes apparent in Fig. 1. At 0 wt% carbon black, the fabricated membranes appeared white, whereas at the highest loading, 62.5 wt%, they were black. Historically, carbon blacks have been utilized as pigments for textiles and ink (Li & Sun, 2007; Wypych, 1999). Thus, the deepening in color displayed by the membranes after each subsequent loading of carbon black is a visual confirmation that an increasing incorporation of carbon black particles has been achieved. After electrospinning the carbon black–chitosan solutions, the membranes were subsequently cross-linked with glutaraldehyde (GA) vapor to increase their chemical stability (Schiffman & Schauer, 2007).

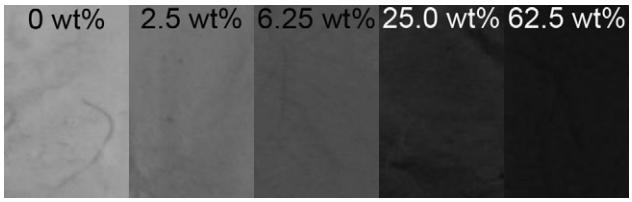

Fig. 1. Digital images of electrospun carbon black–chitosan membranes display an apparent deepening of color which qualitatively confirms that an increasing concentration of carbon black has been incorporated within the fibers. From left to right, 0–62.5 wt% carbon black. Weight percent was calculated in reference to the initial mass of chitosan.

FESEM determined that all cross-linked electrospun membranes consisted of fine, continuous, randomly accumulated fibers. Cross-linking does not alter the fiber morphology (Schiffman & Schauer, 2007). The micrograph in Fig. 2A displays a cross-linked chitosan membrane, which did not contain any carbon black. These fibers all appear to be cylindrical and were determined to have an average fiber diameter of 172 ± 75 nm. Fig. 2B is a composite membrane loaded with 2.5 wt% carbon black, the lowest weight percent loading evaluated in this study. Chitosan can be used to help disperse carbonaceous materials, such as multiwall carbon nanotubes (Iamsamai, Hannongbua, Ruktanonchai, Soottitantawat, & Dubas, 2010). Therefore, at the lower concentration of carbon black, we hypothesize that 66.9 ± 16.2 nm diameter particles are relatively well dispersed by the chitosan. These fibers appeared to have a similar morphology to the ones that did not contain any carbon black. In general, individual fibers were smooth and continuous. Their average fiber diameter was 234.5 ± 180.5 nm. The average

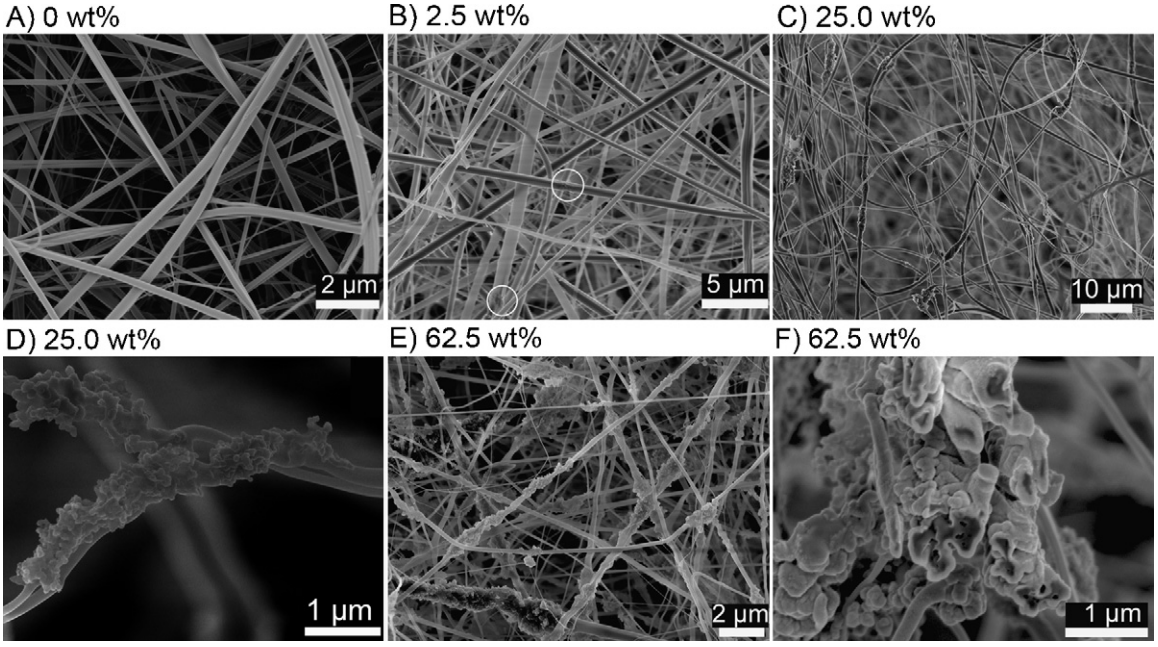

Fig. 2. FESEM micrographs displaying cross-linked electrospun chitosan membranes fabricated with (A) 0 wt%, (B) 2.5 wt%, (C and D) 25.0 wt%, and (E and F) 62.5 wt% carbon black. Small agglomerations of carbon black are observed within the white circles in micrograph (B). For micrographs (A–E), bulk electrospun fibers were imaged; whereas for (F), FIB milling was conducted to elucidate a cross-sectional view of a carbon black–chitosan membrane.

and standard deviation was larger than that of the pure chitosan membranes, which can be attributed to the few instances wherein the incorporated carbon black was apparent, circles in Fig. 2B. In these instances, close investigation reveals that the fibers have a wrinkled and bumpy morphology.

Micrographs displaying the overall and an expanded region of the fiber morphology present in membranes electrospun from 25.0 wt% carbon black–chitosan solutions are displayed in Fig. 2C and D, respectively. Herein, changes in the fiber morphology due to the incorporation of carbon black particles are apparent. At this weight loading, the fibers lose their smooth cylindrical shape in the regions where the agglomerates have formed. Agglomerations of carbon black particles are visually present parallel with the long-axis of individual fibers. At 25.0 wt% carbon black incorporation, the average fiber diameter was determined to be 396.6 ± 216.9 nm. In Fig. 2D, there are fibers within the membranes, which measure approximately 100 nm in diameter; these areas may or may not contain carbon black nanoparticles. The fiber diameters wherein carbon black is agglomerated measure up to 700 nm in diameter. Cross-linked membranes containing 62.5 wt% carbon black are displayed in Fig. 2E. The fibers within these membranes displayed the largest amount of variation in terms of both fiber diameter and agglomeration. Specifically, some of the fibers within this membrane remain very thin 100 nm, while occasionally others display larger agglomerations of carbon black than observed at lower carbon black loadings. For instance, the fiber imaged at the bottom left of Fig. 2E measures 1.5 μm in diameter at its widest point. In reference to the variation in agglomeration, the carbon black either appears as a small clump, along a fiber (similar to the 25.0 wt% loading), or as a very large agglomeration along the fiber axis. As a result of this variation, calculating a meaningful average fiber diameter was not possible.

The micrograph in Fig. 2F is of a 62.5 wt% carbon black–chitosan membrane, which has been FIB milled to reveal the cross-section of individual fibers. The micrograph displays that within the fibers, the carbon black nanoparticles agglomerate. Between the agglomerates, significant porosity (black spots) is observed. We hypothesize that the carbon black nanoparticles are effectively held in place and housed within a shell of the chelating chitosan matrix. These hypotheses are further supported in following section.

Chuangchote, Sirivat, and Supaphol (2007) reported that the incorporation of up to 10 wt% carbon black into electrospun poly(vinyl alcohol) fibers did not alter the FTIR spectra or XRD pattern of the membranes. However, we observe changes in both the FTIR spectra at 2.5 wt% and XRD pattern at 6.25 wt% loading of carbon black, Figures S3 and S4, respectively.

We hypothesize that the chitosan is chelating carbon black particles, yet retaining enough free amine groups to allow for cross-linking to ensue. Upon the incorporation of as low as 2.5 wt% carbon black nanoparticles, we observe the formation of a split peak at 1260 cm^{-1} due to the bending vibration of the O–H groups (Wang, Du, & Fan, 2005). Successful cross-linking by the GA-vapor to the carbon black–chitosan membranes is confirmed the disappearance of the C=N imine peak at 1560 cm^{-1}; thus indicating that a Schiff base imine functionality has occurred due to a loss of the free amine peak (Schiffman & Schauer, 2007; Tual, Espuche, Escoubes, & Domard, 2000).

XRD conducted on carbon black powder displayed a broad peak at $2\theta = 26.08^{\circ}$ (having a d-spacing of 3.41 Å). This peak is consistent with previous findings (Lalande et al., 1995) and did not interfere with the five commonly observed crystalline reflections (0 2 0), (1 1 0), (0 4 0), (1 2 0), and (1 3 0) that chitosan displays for 2θ values between 5° and 27° (Feng, Liu, & Hu, 2004; Wada & Saito, 2001). Diffraction patterns of 2.5 wt% carbon black–chitosan membranes displayed the same peak locations and intensities as pure chitosan membranes (Schiffman et al., 2009). However, upon increased carbon black loading to 6.25 wt% or greater, all diffraction peaks were lost as displayed in Figure S4. This indicates that there is a difference in the amount of carbon black between the low and higher carbon black loaded membranes.

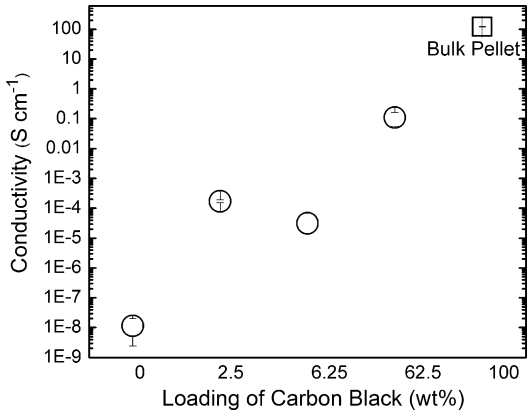

Fig. 3. Plot displays the conductivity (σ) of electrospun carbon black–chitosan membranes and bulk carbon black pellet. Average conductivity values were determined by testing at least three different electrospun membranes. Standard deviation is displayed.

3.3. Performance of electrospun carbon black–chitosan membranes

Chemical stability studies revealed that all as-spun (non-cross-linked) membranes disintegrated instantly upon contact with acidic and aqueous solutions. However, cross-linked carbon black–chitosan membranes were robust when immersed in acidic, basic, and aqueous solutions for 20 days. Time intervals longer than 20 days were not tested. All loadings: 0, 2.5, 25.0, 50.0, and 62.5 wt% carbon black behaved similarly after the 15 min, 72 h, and 20-day evaluations. All membranes could be removed from the solutions and exhibited shape and color retention. Additional visual inspection of the remaining solutions from which they were removed did not indicate a color change, or any signs that carbon black from the fibrous membranes was present. It should be noted that since carbon black is a powerful dye, solutions which contain a very low amount, 0.03 g/30 mL or 0.1 wt% of carbon black nanoparticles still visually appear to have particles in them (image not shown). Hence, we believe that the carbon black, even at a 62.5 wt% loading, is in fact incorporated and immobilized in the electrospun membranes.

The electrical conductivity (σ) of the thin, flexible carbon black–chitosan membranes, was determined by measuring their resistance (R) utilizing AC impedance spectroscopy and taking into account the thickness and cross-sectional area of the membrane. Table S1 displays average membrane thicknesses and conductivity. Reliable resistivity data was repeatedly acquired on the plane normal to the electrospun membranes. Conductivity data could be categorized into three ranges, which increased as a function of carbon black content, see Fig. 3. Pure chitosan membranes, i.e. 0 wt% carbon black were found to have conductivities on the order of $1.14 \times 10^{-8} \pm 9 \times 10^{-9}$ S cm^{-1}. Membranes that contained 2.5 wt% or 6.25 wt% carbon black had conductivities three orders of magnitude higher, and membranes that contained 62.5 wt% carbon black had conductivities of 0.109 ± 0.05 S cm^{-1}. For comparison, the conductivity of a 6.5 mm thick carbon black pellet, which was hard packed without the use of potassium bromide (KBr) or other chemicals was determined to be 119.0 ± 0.2 S cm^{-1}. When taking the conductivities of the electrospinning solutions, the chitosan to TFA solvent ratio played a key role. However, during the electrospinning process, most of the solvent evaporates (Schiffman & Schauer, 2008). While remnant TFA might be present, this value would be constant in all membranes.

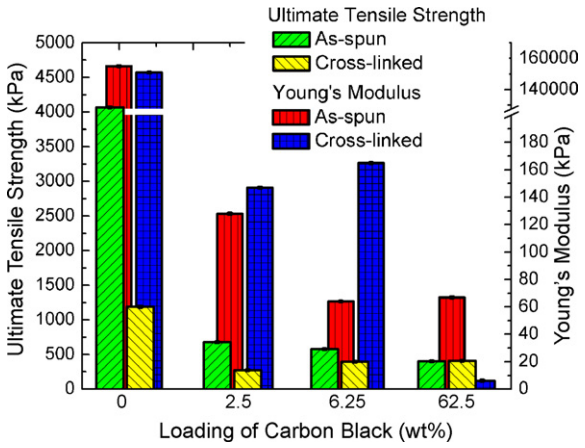

Fig. 4. Bar graphs display the average ultimate tensile strength (left axis) and Young's modulus (right axis) of as-spun and cross-linked electrospun carbon black–chitosan membranes. Three samples were averaged for each measurement, standard deviation is displayed but small.

It is also known that the electrical properties of carbon black–polymer composites vary dramatically as a function of the dispersion, shape, and orientation of the carbon black particles. It is important to note that chitosan is an insulating polymeric material and thus tunneling will be prevented in the fiber areas that do not contain carbon black, where the carbon black particles are too disperse, or whenever the polymer shell around the carbon black is too thick (Balberg, 2002).

The mechanical properties of electrospun composite membranes are a function of a number of factors, including the constituents of the composites, the structure of the fibers, bonding between the fibers, orientation of the fibers within the membrane, and the movement of the individual fibers past one another. Due to the method of analysis used, the mechanical properties of the membrane as a whole are obtained, rather than that of the individual fibers (Lee, Kim, Ryu, Kim, & Choi, 2003; Wang, Jin, Kaplan, & Rutledge, 2004).

Figs. 4 and 5 display the results of the uniaxial tensile testing of as-spun and cross-linked carbon black–chitosan membranes. Upon the incorporation of carbon black into the chitosan membranes, all mechanical properties were found to decrease. This was not surprising since a key reason for decreasing the percolation threshold within conductive polymer composites is to retain mechanical properties (Dai, Xu, & Li, 2007). Nevertheless, the extent

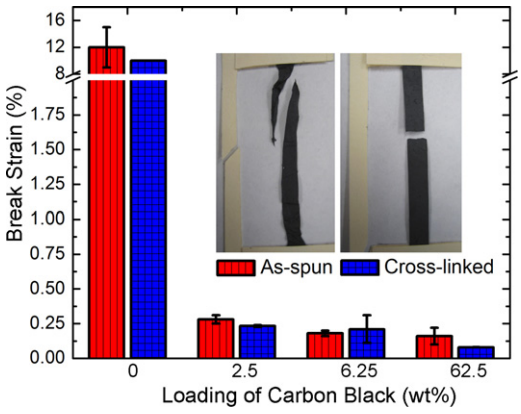

Fig. 5. Displays average break strain (%) of as-spun and cross-linked electrospun carbon black–chitosan membranes. Three samples were averaged for each measurement, standard deviation is displayed. Inset digital images display the breaking behavior observed for all as-spun and cross-linked carbon black–chitosan membranes.

to which the incorporation of carbon black nanoparticles decreased the mechanical properties was of interest. Ultimate tensile strength decreased by an order of magnitude for both the as-spun and the cross-linked membranes. Additionally, much lower break strains were observed for all carbon black containing membranes. For example, the as-spun break strain was $12 \pm 0.3\%$, whereas for as-spun fibers containing 2.5 wt% carbon black it was $0.28 \pm 0.03\%$.

When the pure chitosan membranes were tested, first the individual fibers randomly aligned along the tensile pull axis, and then experienced an increase in the allowable stresses until failure (Schiffman & Schauer, 2007). This increase is a result of the large number of fiber-to-fiber contacts, which intrinsically provided a high cohesive force. The decrease in mechanical properties that the as-spun carbon black–chitosan membranes displayed could be a result of the rigid carbon black nanoparticles acting as defects. Possibly, there was poor interfacial bonding (Chuangchote et al., 2007; Supaphol, Harnsiri, & Junkasem, 2004) between individual fibers, as was supported by the visual appearance of how the as-spun membranes failed. The inset digital images in Fig. 5 are of as-spun and cross-linked 62.5 wt% carbon black–chitosan membrane samples post-mechanical testing. The "C" shaped sample holder is close to its original position; the initial gauge length and sample width were 5.0 cm and 0.5 cm, respectively. The carbon black may have caused a planar shearing, rather than the membrane experiencing a strong bonding between the fibers prior to their breaking during the uniaxial tensile test. This layer shearing occurred for all as-spun carbon black–chitosan membranes, thus supporting the theory of weak interfacial bonding within the composite. Also, FIB micrographs demonstrated that individual fibers are porous, which also could decrease the bulk mechanical properties.

The cross-linked carbon black–chitosan membranes did not shear into layers and their stress-strain curves exhibited a distinct maximum. This was due to the fact that cross-linking of the fibers with GA-vapor restricted them from slipping past each other since they were point-bonded together.

Chuangchote et al. (2007) and Hwang et al. (2007) have mechanically tested electrospun membranes of poly(vinyl alcohol)–carbon black (0–10 wt%) and PU elastomer (Pellethane 2103-70A)–carbon black (0–9.46 wt%), respectively. Chuangchote et al. found that membranes containing 8 wt% carbon black had the highest Young's modulus (162.2 ± 37.4 MPa) whereas Hwang et al. found that the 9.46 wt% carbon black had the highest value (3.75 ± 0.86 MPa). The Young's modulus of Chuangchote et al.'s and Hwang et al.'s membranes before the addition of carbon black were 80.6 ± 27.2 MPa and 0.74 ± 0.16 MPa, respectively. The highest tensile strength value was reported for 3.65 wt% carbon black for Hwang's elastomer (7.48 ± 1.02 MPa). However, Chuangchote et al. noted that PVA membranes, similar to our chitosan ones, containing no carbon black had the highest tensile strength (7.37 ± 2.7 MPa). Finally, in agreement to our findings, both studies determined that pure membranes, i.e., which did not contain any carbon black exhibited the highest elongation at break ($162.2 \pm 37.4\%$ for Chuangchote et al. and $613.51 \pm 32.06\%$ for Hwang et al.).

4. Conclusion

For the first time, the successful electrospinning of carbon black–chitosan membranes have been demonstrated and their morphological and chemical changes studied. The conductivity of the thin, flexible membranes increased from $1.14 \times 10^{-8} \pm 9 \times 10^{-9}$ S cm^{-1} to 0.109 ± 0.05 S cm^{-1} by increasing the concentration of carbon black within the natural polymer fibers from 0 to 62.5 wt%. After cross-linking, the fabricated carbon black–chitosan membranes exhibited chemical stability for 20 days in aqueous, acidic, and basic solutions.

Acknowledgements

JDS thanks the NSF-Integrative Graduate Education and Research Traineeship (NSF IGERT) (DGE-0221664) and Graduate Assistance in Areas of National Need-Drexel Research and Education in Advanced Materials (GAANN-DREAM) (P200A060117), which is funded by the Department of Education's Office of Postsecondary Education for funding. CLS thanks the Nanotechnology Institute Proof of Concept grant for funding. For the assistance and instruction with AC impedance spectroscopy, the authors thank Daniel T. Hallinan and Yossef A. Elabd. Additionally, the authors thank Ulrike Eigenthaler and Michael Hirscher, MPI for Metals Research, Stuttgart, Germany for their expert advice and support in the preparation of FIB cross-sections.

Appendix A. Supplementary data

Supplementary data associated with this article can be found, in the online version, at doi:10.1016/j.carbpol.2011.01.013.

References

Balberg, I. (2002). A comprehensive picture of the electrical phenomena in carbon black–polymer composites. *Carbon*, *40*(2), 139–143.

Chen, S. G., Hu, J. W., Zhang, M. Q., Li, M. W., & Rong, M. Z. (2004). Gas sensitivity of carbon black/waterborne polyurethane composites. *Carbon*, *42*(3), 645–651.

Chuangchote, S., Sirivat, A., & Supaphol, P. (2007). Mechanical and electrorheological properties of electrospun poly(vinyl alcohol) nanofibre mats filled with carbon black nanoparticles. *Nanotechnology*, *18*(14), 145705.

Dai, K., Xu, X.-B., & Li, Z.-M. (2007). Electrically conductive carbon black (CB) filled in situ microfibrillar poly(ethylene terephthalate) (PET)/polyethylene (PE) composite with a selective CB distribution. *Polymer*, *48*(3), 849–859.

Doleman, B. J., Lonergan, M. C., Severin, E. J., Vaid, T. P., & Lewis, N. S. (1998). Quantitative study of the resolving power of arrays of carbon black–polymer composites in various vapor-sensing tasks. *Analytical Chemistry*, *70*(19), 4177–4190.

Elabd, Y. A., Walker, C. W., & Beyer, F. L. (2004). Triblock copolymer ionomer membranes. Part II. Structure characterization and its effects on transport properties and direct methanol fuel cell performance. *Journal of Membrane Science*, *231*(1–2), 181–188.

Feng, F., Liu, Y., & Hu, K. (2004). Influence of alkali-freezing treatment on the solid state structure of chitin. *Carbohydrate Research*, *339*(13), 2321–2324.

Hasegawa, M., Isogai, A., Onabe, F., & Usuda, M. (1992). Dissolving states of cellulose and chitosan in trifluoroacetic acid. *Journal of Applied Polymer Science*, *45*(10), 1857–1863.

Hwang, J., Muth, J., & Ghosh, T. (2007). Electrical and mechanical properties of carbon-black-filled, electrospun nanocomposite fiber webs. *Journal of Applied Polymer Science*, *104*(4), 2410–2417.

Iamsamai, C., Hannongbua, S., Ruktanonchai, U., Soottitantawat, A., & Dubas, S. T. (2010). The effect of the degree of deacetylation of chitosan on its dispersion of carbon nanotubes. *Carbon*, *48*(1), 25–30.

Krajewska, B. (2004). Application of chitin- and chitosan-based materials for enzyme immobilizations: A review. *Enzyme and Microbial Technology*, *35*(2–3), 126–139.

Kumar, M. N. V. R. (2000). A review of chitin and chitosan applications. *Reactive and Functional Polymers*, *46*(1), 1–27.

Kurita, K. (2006). Chitin and chitosan: Functional biopolymers from marine crustaceans. *Marine Biology*, *8*, 203–226.

Lalande, G., Cote, R., Tamizhmani, G., Guay, D., Dodelet, J. P., Dignard-Bailey, L., et al. (1995). Physical, chemical and electrochemical characterization of heat-treated tetracarboxylic cobalt phthalocyanine adsorbed on carbon black as electrocatalyst for oxygen reduction in polymer electrolyte fuel cells. *Electrochimica Acta*, *40*(16), 2635–2646.

Lee, K. H., Kim, H. Y., Ryu, Y. J., Kim, K. W., & Choi, S. W. (2003). Mechanical behavior of electrospun fiber mats of poly(vinyl chloride)/polyurethane polyblends. *Journal of Polymer Science, Part B: Polymer Physics*, *41*(11), 1256–1262.

Li, D., & Sun, G. (2007). Coloration of textiles with self-dispersible carbon black nanoparticles. *Dyes and Pigments*, *72*(2), 144–149.

Pedicini, A., & Farris, R. J. (2004). Thermally induced color change in electrospun fiber mats. *Journal of Polymer Science, Part B: Polymer Physics*, *42*(5), 752–757.

Rinaudo, M. (2006). Chitin and chitosan: Properties and applications. *Progress in Polymer Science*, *31*(7), 603–632.

Rinaudo, M., Pavlov, G., & Desbrières, J. (1999). Influence of acetic acid concentration on the solubilization of chitosan. *Polymer*, *40*(25), 7029–7032.

Schiffman, J. D., & Schauer, C. L. (2007). Cross-linking chitosan nanofibers. *Biomacromolecules*, *8*(2), 594–601.

Schiffman, J. D., & Schauer, C. L. (2008). A review: Electrospinning of biopolymer nanofibers and their applications. *Polymer Reviews*, *48*(2), 317–352.

Schiffman, J. D., Stulga, L. A., & Schauer, C. L. (2009). Chitin and chitosan: Transformations due to the electrospinning process. *Polymer Engineering & Science*, *49*(10), 1918–1928.

Supaphol, P., Harnsiri, W., & Junkasem, J. (2004). Effects of calcium carbonate and its purity on crystallization and melting behavior, mechanical properties, and processability of syndiotactic polypropylene. *Journal of Applied Polymer Science*, *92*(1), 201–212.

Tiwari, M. K., Yarin, A. L., & Megaridis, C. M. (2008). Electrospun fibrous nanocomposites as permeable, flexible strain sensors. *Journal of Applied Physics*, *103*(4), 044305.

Tual, C., Espuche, E., Escoubes, M., & Domard, A. (2000). Transport properties of chitosan membranes: Influence of crosslinking. *Journal of Polymer Science, Part B: Polymer Physics*, *38*(11), 1521–1529.

Wada, M., & Saito, Y. (2001). Lateral thermal expansion of chitin crystals. *Journal of Polymer Science, Part B: Polymer Physics*, *39*(1), 168–174.

Wang, Q., Du, Y. M., & Fan, L. H. (2005). Properties of chitosan/poly(vinyl alcohol) films for drug-controlled release. *Journal of Applied Polymer Science*, *96*(3), 808–813.

Wang, M., Jin, H. J., Kaplan, D. L., & Rutledge, G. C. (2004). Mechanical properties of electrospun silk fibers. *Macromolecules*, *37*(18), 6856–6864.

Wypych, G. (1999). Sources of fillers, their chemical composition, properties, and morphology. *Handbook of fillers* (pp. 15–202). New York: William Andrew Inc.

Zhang, M. Q., & Zeng, H. M. (1997). Conducting thermoplastics composites. In O. Olabisi (Ed.), *In Handbook of thermoplastics* (pp. 873–891). New York: CRC Press.